MECHANIKA TEORETYCZNA
I STOSOWANA
Journal of Theoretical
and Applied Mechanics
4, 30, 1992

FINITE ELEMENT ANALYSIS OF ELASTIC–PLASTIC PLANE CONTACT PROBLEM WITH NONLINEAR INTERFACE COMPLIANCE

RYSZARD BUCZKOWSKI

Technical University of Szczecin

MICHAŁ KLEIBER

Institute of Fundamental Technological Research, Warsaw

A solution to the two–dimensional elastic–plastic contact problem taking into account the deformation of the surface roughness at the contact zone is presented. The problem has been described using an incremental variational functional followed by the approximation typical of the element displacement method. A special contact element composed of three discrete spring elements has been used for the simulation of nonlinear properties on the contact surface. The stiffness of these spring elements has been determined on the basis of some empirical mechanical characteristics of the contact flexibility of rough surfaces. The correctness of the algorithm presented has been illustrated by a computational example. The influence of parameters defining the contact compliance on the distribution of stresses and displacements on the contact surface is discussed.

1. Introduction

The classical tool for the analysis of elastic contact problem is the Hertz's theory put forward in 1881. However, this method does not allow for analysis of complicated problems, especially bodies with various complex geometries and geometrical and physical nonlinearities both in the contact zone and inside the contacting bodies. In recent years large–scale computational techniques have been developed, the most promising among them being undoubtfully the finite element method. Most numerical investigations in the field of contact mechanics have been restricted to Signiorini's unilateral impenetrability conditions (which may be relevant for very hard and smooth contact surfaces) and the classical friction model. The classical friction law of dry sliding (ideal Coulomb's law) can be summarized as follows: the coefficient of proportionality, known as the coefficient

of friction, is independent of the apparent area of contact as well as of roughness and relative velocity in tangential motion, and the friction forces are proportional to the normal contact forces.

Real surfaces are always rough; a machined surface is composed of micro–asperities. As a result, when two surfaces approach each other contact occurs first at the tops of the highest asperities. When the load is increased the asperities are crushed and the surfaces sink together. We say that the interface compliance has occured. The surface roughness of the joint has a significant effect on the contact stiffness as it determines the global behaviour of the machine joint. To take into account the influence of roughness upon the contact pressure and shear stress distribution different analysis methods may be used. Some methods are based on the discrete model in which the asperities have simple geometrical forms, e.g. that of a cylinder, wedge, sphere, etc. In these methods the analysis resolves itself into the investigation of influence of the microgeometrical morphology and mechanical material propertities on the interaction of the contacting rough surfaces (Tangena and Wijnhoven (1985); Salamon, Tong, Mahmoud (1985); Plesha and Belytschko (1986); Morawski, Rakowski and Skalski (1986); Skalski (1988) or Yamada and Kakubari (1988). Another approach to the analysis of the contact problem consists in the experimental determination of the load–displacement characteristics for real surfaces and the substitution of simple mathematical expressions for them. Such a method has been employed in the present study. Back, Burdekin and Cowley (1973a) were the first who used experimentally determined parameters (normal compliance condition) in the calculation of examples of simple machine tool joints by the finite element method. In their work the authors stated that it was not necessary to know precise values of the normal compliance parameters for a sufficiently accurate solution; some differences in the values of the parameters c_N and m (see the next section) were giving very small errors in the total normal surface deflections. According to those authors, the calculation of the normal stiffness and pressure distribution in the joints under the assumption that the structural components are rigid gives the normal displacements several times smaller than those obtained with a normal compliance. Even for a very low interface pressure the errors obtained when assuming rigid components were large and increasing with the increase of the interface pressure. The same authors (1973b) presented three iterative methods of simulation of the surface roughness: the spring, plate and hydrostatic method. When the methods described in their work are compared, each of them presents some advantages over the other depending upon a particular problem to be solved. In the case of a large relative displacement of the pair of nodes in contact in the tangential direction to the surface, the spring method was recommended (a tangential stiffness must then be introduced). Chvorostuchin et al. (1980; 1981) used the finite element method to solve the press–fit joint with surface roughness in the presence of waviness deviations after machi-

ning operations. In Kops and Abrams (1984) the additional effect of the shear and normal stiffness of the interface on the thermal deformation of machine tool structure was discussed. An effective model of frictional interface behaviour was proposed by Villanueva–Leal and Hinduja (1984). These authors were first to successfully employ the incremental formulation to solve 3D–bolted joints with both the normal and tangential contact stiffness. They limited the values of shear forces by the Coulomb's law of friction. The elastic–plastic plane contact problem with the contact stiffness was first presented by Bloch and Orobinski (1983). These authors used the elastic–plastic shear relations by Reshetov and Kirsanova (1970) and assumed the ideal friction law. A single bolted joint was analysed by Kawiak (1984) who also presented a solution to 3D–bolted model. Unfortunately, however, the 20–nodal–hexahedral finite elements together with the spring contact elements lead to erroneous numerical results (Gabbert, 1987). The problem of loading and unloading of a flat circular punch contacting a half space was solved by Klarbring (1986) by using mathematical programming (parametric linear complementarity method). A linear normal model of the contact interface ($m = 1$, see section 2) and a generalized hardening Coulomb friction was there assumed. Based on the analysis of some experimental results, Oden and Martins (1985); Martins and Oden (1986) and Martins, Oden and Simoes (1990) gave a variational formulation (variational inequalities with a regularisation of the friction functional) for the dynamic problem and solved it using finite element procedures. The existence and uniqueness of solution to the contact problem with non–linear compliance of a metallic body were proved by Rabier et al. (1987), Klarbring et al. (1988; 1990). Wriggres (1987) and Wriggers, Vu–Van and Stein (1990) took advantage of the expressions describing the non–linear behaviour of the contact surface in the normal and tangential direction. They reported the solution to two–dimensional static and dynamic problems under large deformations and a non–linear friction law. Cheng and Kikuchi (1985a; 1985b) presented an elastic–plastic problem of unilateral contact in which the elastic–plastic friction law was extended to large deformations typical of some metal forming processes. Altenbach and Buczkowski (1991) carried out an incremental finite element analysis of an elastic, two–dimensional, axisymmetrical contact problem taking account of non–linear properties of the contact zone. To limit the value of tangential forces Fredriksson's friction law was introduced.

The present study deals with the solution to a plane stress and plane strain elastic–plastic contact problem with linear hardening. The nonlinear problem is solved by using an incremental–iterative modified Newton–Raphson procedure. A flat elastic punch pressed into the elastic–plastic foundation is analysed as a numerical example. The structure is discretized by the eight node quadratic element of the serendipity family. In what follows the elastic–plastic behaviour at the contact interface is designated by $(e$–$p)$ whereas the elastic–plastic deformation of the contacting bodies A and B by $(E$–$P)$.

2. Modelling of interface surface roughness

2.1. Normal behaviour

Many researchers have observed that in the presence of surface asperities the relationship between the interface pressure and the approach of the surfaces in contact can be expressed by the following nonlinear power equation (Back, Burdekin and Cowley, 1972; Oden and Martins, 1985; Levina, 1967)

$$u_N = c_N p_N^m \tag{2.1}$$

where u_N is the deflection of the asperities, p_N is the mean interface pressure and the parameters c_N and m are coefficients depending upon the materials in contact, matching process, height of the asperities, relative orientation at the surface layers, hardness, flatness deviation and size of the contact area, respectively.

For different surface finishes and material combinations the values of c_N and m were given by Back et al. (1973). The parameters c_N and m vary from 0.3 to 2.0 and from 0.3 to 0.7, respectively. For most metallic materials the parameter c_N is proportional to the modulus of elasticity whereas m is usually equal to 0.5. As suggested by Levina (1967) and Martins, Oden and Simoes (1990), these coefficients are applicable up to the contact pressure of 5 [MPa]. For a higher pressure range (from 0.8 [MPa] to 31 [MPa]) Connolly and Thornley (1968) formulated an expotential law

$$p_N = a\mathrm{e}^{bu_N} \tag{2.2}$$

where a, b are the coefficients which depend upon the surface finish and the material combinations.

Taniguchi at el. (1984) proposed and experimentelly verified a linear relation for the contact stresses and the surface approach for a heigh pressure range over 10 [MPa] up to 100 [MPa] in the form

$$u_N = Ap_N + B \qquad p_N \geq p_c \cong 10\ [\mathrm{MPa}] \tag{2.3}$$

where the coefficient A extends from 0 to 10 [nm/MPa] and the coefficient B extends from 0 to 40 [μm]; p_c is called the critical interface pressure. The corresponding coefficients c_N and m in Eq (2.1) are evaluated for $p_N < p_c$.

In the field of engineering, there exist structures like plastic–injection molds or bolted, machine–tool and shrink–fit joints which are subject to a pressure over 100 [MPa]; it has not been cleared whether the equation can be applied to a much higher contact pressure range while it is necessary to investigate the relationship between the critical pressure and the surface roughness to know which of the equations may be employed in the computational process.

Experiments indicate that the higher contact pressure the steeper the contact normal stiffness characteristics. At the same time the contact stiffness increases; $k_N = (\partial p_N / \partial u_N) \to \infty$. This fact can be ensured by taking $c_N \to 0$. In the present computational procedure it is assumed that $c_N = 0.001$ and $m = 0.5$.

2.2. Tangential behaviour

In addition to normal loads the joint may be subject to tangential loading. The behaviour of an interface loaded in the tangential direction was studied by Courtney-Pratt and Eisner (1957), Kirsanova et al. (1967, 1970), Masuko et al. (1974), Koizumi et al. (1979) and recently by Thornley and Elewa (1988). The experiments showed that both the relative displacement of the two bodies and the area of contact between them were smooth, increasing functions of the tangential force as long as this force was increasing monotonically from zero. It was measured that the relative displacement of two metallic bodies in contact was increasing with frictional force t_T, tending to infinity as t_T was approaching asymptotically a value of $t_{max} = \mu_m t_N$, at which the threshold of macroslip (continued sliding) was reached. The value of μ_m defined and found in this way agrees well with the values of the coefficients of static friction. Release and even reversal of the tangential force produces no further irreversible changes until the force is increased again, in either direction, to a numerical value as heigh as the highest one previously reached.

In this study the nonlinear behaviour has been approximated by two straight lines (elastic and plastic part) (Reshetov and Kirsanova, 1970) as follows

$$u_T = u_T^e + (k_T^p)^{-1}(p_T - p_T^Y) \tag{2.4}$$

where u_T^e is the elastic shear displacement, k_T^p is the shear-plastic stiffness coefficient, p_T^Y denotes elastic limit for shear stress or initial yielding at the surface and p_T is the actual shear-stress.

It was found (Reshetov and Kirsanova, 1970) that for repeated loads which did not exceed the first loading limit the displacements were only elastic. It was also observed that at the elastic limit the ratio of shear stress p_T^Y to the normal pressure p_N was approximatelly half of the coefficient of the static friction μ_m

$$\frac{p_T^Y}{p_N} = \mu_Y = \frac{1}{2}\mu_m \tag{2.5}$$

Experiments of Courtney-Pratt and Eisner (1957) and Oden and Martins (1985) suggested that the preliminary displacements were essentialy irreversible (plastic). This apparently holds true for the soft materials (gold, platinium, tin, indium) only. Koizumi et al. (1979) taking into account the bolted joints as an

example of jointed surface under a relatively high normal contact pressure found that the soft material (such as aluminium) displayed a large micro–slip (plastic displacement) and a hard mild steel displayed a relatively small micro–slip. Experiments of Koizumi et al. (1979) indicated that the tangential elastic displacement u_T^e decreased with an increase of the preload. An interesting observation is that the elastic displacement is proportional to $\mu_F = t_T/t_N$ with the proportionality coefficient depending on materials type, hardness, roughness and apparent contact area of the joined surfaces. Thornley and Elewa (1988) in the framework of experiments on shrink–fitted joints reported that the tangential displacement was increasing almost linearly with the applied tangential load during the loading cycles for large interference values. The value of interference plays an important role in determining the magnitude of tangential displacement between the joint matching surfaces. When the tangential load reaches a magnitude equivalent to the joint holding load, gross–slip (macro–slip, sliding) occurs and the joint can no langer be considered shrink–fitted.

It was found that the elastic displacement took place within the specific range of loads. For a further increase in the shear force exceeding the limit, the resulting displacements are elastic–plastic followed by macro–slip. Failure of the joint can be generally determined on the basis of the coefficient of limited friction. It was also noticed that elastic displacement of shrink–fitted joints during unloading was about 90% of the overall tangential displacement for large value of interferences. Therefore, the elastic displacement can be taken to represent the tangential displacement of the shrink–fitted joint with a large value of interference. Some authors have suggested that it is necessary to design the joint in such a way that the tangential deformations remain below the plastic limit. Reshetov and Kirsanova (1970) and Masuko (1974) found that shear stiffness depended upon the surface finish and that it was decreasing with the decrease of the normal pressure. The results obtained by Reshetov and Kirsanova (1970) indicate that the relationship between the shear stiffness and the normal interface pressure can be presented as (Back et al. (1973a))

$$k_T^e = \frac{p_N{}^S}{R} \tag{2.6}$$

where S and R are again parameters dependent upon the pair of materials and surface finish (Back et al. (1973a)).

2.3. Normal stiffness during loading

The direct iterative procedures cannot lead to an acceptable solution to the interface problem because they do not follow the stiffness variation at the interface as given by Eq (2.1). The use of the incremental method is thus unavoidable be-

cause it makes it possible to gradually adjust the slope so that the resultant curve $u_N - p_N$ follows the desired experimental curve. The stiffness value corresponds to the slope of the pressure–deflection characteristics at the working interface pressure. Using the power law relationship in Eq (2.1) gives stiffness per unit area as

$$k_N = \frac{dp_N}{du_N} = \frac{p_N{}^{(1-m)}}{c_N m} \tag{2.7}$$

where p_N is the total interface pressure acting at the contact node and c_N, m are coefficients.

For the first load increment (iteration) the slope of the curve $u_N - p_N$ cannot be used because its value is zero at the origin. Hence the normal stiffness per unit area at this point on the interface for the first iteration is computed using the secant

$$k_N^{[1]} = \frac{\Delta p_N^{[1]}}{\Delta u_N} = \frac{p_m}{\Delta u_N} \tag{2.8}$$

where p_m is the uniform pressure across the interface. Using Eq (2.1) we obtain

$$k_N^{[1]} = \frac{(p_m)^{1-m}}{c_N} = \left(\frac{\Delta f_N^{[1]}}{c_N A_c}\right)^{1-m} \tag{2.9}$$

where $\Delta f_N^{[1]}$ is the incremental load for the first iteration and A_c is the apparent area of contact.

Since the value of k_N at the first iteration is calculated using the secant, the first incremental load $\Delta f_N^{[1]}$ is chosen to be small (about 5 per cent of the total load). The greater the initial load the greater the error incurred at the first iteration (Villanueva–Leal and Hinduja, 1984).

For the second and next load increments loads the pressure can be calculated as (Altenbach and Buczkowski, 1991)

$$p_{Nj}^{[i]} = \frac{k_N^{[i]}\left(\Delta u_{Nj}^{[1]} + \sum_{l=2}^{i} \Delta u_N^{[i]}\right)}{a_j} \tag{2.10}$$

and the normal stiffness is evaluated from the slope of the pressure–deflection curve (Eq (2.7)) as

$$k_{Nj}^{[i]} = \frac{\left(p_{Nj}^{[i-1]}\right)^{1-m}}{c_N m} a_j \tag{2.11}$$

where j is the number of a contact element, a_j is the area of influence and i denotes the iteration number.

This approximation is valid only if the normal pressure remains constant. If during the iteration process a contact element is subject to tension it means that

loading has begun. For the discussion of this case the reader is referred to Altenbach and Buczkowski (1991). The point will stay in contact as long as the resultant contact pressure p_N updated by Δp_N remains negative. When the resultant pressure does not satisfy $p_N \leq 0$ the contact stiffness submatrices are removed from the global stiffness matrix. This indicates that a certain part of the interface area has lost contact.

2.4. Tangent stiffness

Due to the irreversible character of the friction phenomena an incremental formulation has been employed. After initial yielding p_T^Y (see Eq (2.4)), we consider a further load resulting in an incremental increase of the tangential stress Δp_T, accompanied by a change of the tangential displacement Δu_T. The tangential displacement can be separated into elastic and plastic components as (see Fig.1)

$$\Delta u_T = \Delta u_T^e + \Delta u_T^p \tag{2.12}$$

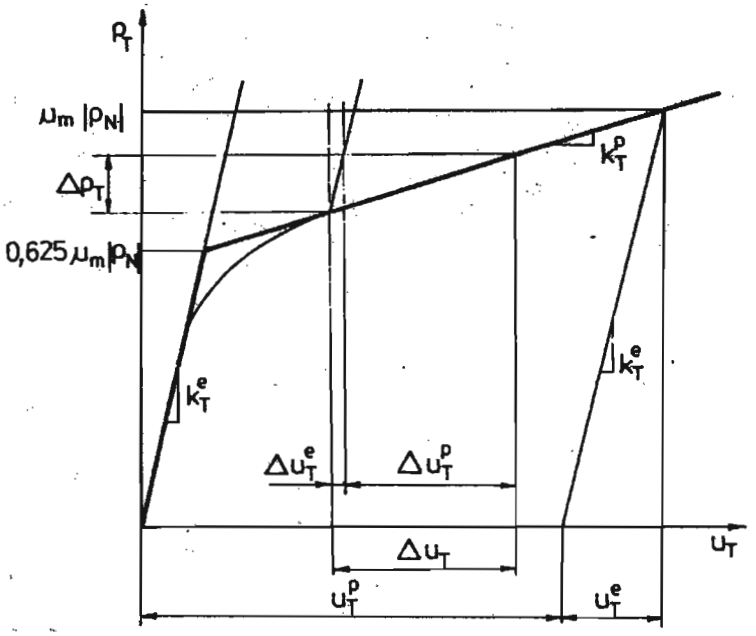

Fig. 1. Tangential contact behaviour in the pre-sliding phase, $k_T^{(e)}$ and $k_T^{(p)}$ are coefficients of the contact stiffness in elastic and plastic range, respectively

Inspired by the classical theory of plasticity the friction hardening modulus H

is expressed as

$$H = \frac{\Delta p_T}{\Delta u_T^p} \tag{2.13}$$

It results from Fig.1 that

$$\begin{aligned} \Delta p_T &= k_T^e \Delta u_T^e \\ \Delta p_T &= k_T^p \Delta u_T \end{aligned} \tag{2.14}$$

where k_T^e and k_T^p are the elastic and the elastic–plastic stiffness coefficients, respectively. Using Eqs (2.12) the relation $(2.14)_2$ takes the form

$$\Delta p_T = k_T^p(\Delta u_T^e + \Delta u_T^p) = k_T^p\left(\frac{\Delta p_T}{k_T^e} + \frac{\Delta p_T}{H}\right) \tag{2.15}$$

Using Eqs (2.13) and (2.15) the friction hardening modulus H can be expressed as

$$H = \frac{k_T^e k_T^p}{k_T^e - k_T^p} \tag{2.16}$$

This can be interpreted as the slope of the tangential stress–displacement curve after removal of the elastic displacement component. In this paper a linear displacement–hardening relationship after reaching p_T^Y has been assumed (Fig.1).

Using Eqs (2.13), (2.16) Δu_T^p is expressed as follows

$$\Delta u_T^p = \Delta p_T\left[(k_T^p)^{-1} - (k_T^e)^{-1}\right] \tag{2.17}$$

By substituting Eqs $(2.14)_1$ and (2.17) into Eq (2.12) we arrive at a complete incremental friction relationship in the form

$$\Delta u_T = \begin{cases} (k_T^e)^{-1}\Delta p_T & \text{for } p_T \le p_T^Y = 0.625\mu_m|p_N| \\ \Delta u_T^e + \Delta p_T\left[(k_T^p)^{-1} - (k_T^e)^{-1}\right] & \text{for } p_T^Y \le p_T \le \mu_m|p_N| \end{cases} \tag{2.18}$$

where μ_m denotes the macroscopic (or static) coefficient of friction and p_T^Y is the elastic shear stress limit.

Under the condition that p_T is smaller than or equal to the shear stress limit p_T^Y the behaviour at the surface interface will be elastic exibiting the stiffness of

$$k_T = \frac{\Delta p_T}{\Delta u_T} = k_T^e \tag{2.19}$$

with k_T^e obtained from Eq (2.6).

Suppose now p_T is increasing until yielding of the surface interface. The tangent stiffness for elastic–plastic behaviour of the surface interface using Eqs (2.12), (2.13) and (2.14) is then given as

$$k_T^{(ep)} = \frac{\Delta p_T}{\Delta u_T} = \frac{\Delta p_T}{\Delta u_T^e + \Delta u_T^p} = k_T^e\left(1 - \alpha \frac{k_T^e}{H + k_T^e}\right) \tag{2.20}$$

where $\alpha = 0$ if $p_T < 0.625\mu_m|p_N|$ (elastic frictional behaviour or frictional unloading) and $\alpha = 1$ if $0.625\mu_m|p_N| \leq p_T \leq \mu_m|p_N|$ (plastic frictional behaviour), μ_m is the static friction coefficient.

In Eq (2.20) the first term represents the elastic stiffness coefficient as given by Eq (2.19). The second term accounts for the stiffness reduction from the elastic value due to yielding. For the perfectly plastic behaviour of contact surface after yielding (Eq (2.16)), $H = 0$ is implied and the elastic–plastic stiffness coefficient $k_T^{(ep)}$ equals zero by Eq (2.20).

2.5. The coefficient of friction

The coefficient of friction was determined experimentally by Lindgren (1973), Müller (1975) and Fredriksson (1975), among others. These experiments were carried out on metallic materials and indicated that coefficient of friction increased with the effective–slip (plastic displacement) u_T^p approaching the macroscopic coefficient of friction μ_m. It was also observed that the coefficient of friction varied with the applied pressure. Higher pressure implied higher maximum coefficient of friction. At lower pressure this effect was not observed. The maximum value of the friction coefficient was observed to be greater for turned contact surfaces than milled ones. In this comparison the contact pressures and surface roughnesses were approximately the same. In view of the results of Fredriksson (1975; 1976) the normalized coefficient of friction may be related to the irreversible (plastic) displacement as

$$\frac{\mu_T}{\mu_m} = 1 - (1 - \beta)e^{(-nu_T^p)} \tag{2.21}$$

where μ_m is again macroscopic (or static) coefficient of friction, β defines the initial coefficient of friction, n is the degree of slip hardening and u_T^p is the accumulated plastic displacement. The parameters should be determined experimentally.

2.6. Friction interface law

By limiting the maximum shear force that can be transmitted through the

joint, the coefficient of friction defines the position at which the tangential loading stops and the macro–slip begins to occur.

We will now introduce a frictional isotropic law (Fredriksson, 1976)

$$f(t_T, t_N, \mu_F) = \|t_T\| + \mu_F t_N \tag{2.22}$$

where t_T and t_N are the tangential and normal contact traction components, respectively and μ_F is the coefficient of friction determined by Eq (2.21).

Assume now that the complete solution is known up to the current state and the conditions on the contact surface at the next increment are of our interest. The slip condition is satisfied if

$$f > 0 \quad \text{or} \quad f = 0 \quad \text{and} \quad \Delta f > 0 \tag{2.23}$$

while the isotropic slip criterion implies that

$$\frac{|t_T|}{|t_N|} > \mu_F \quad \text{or} \quad \frac{|t_T|}{|t_N|} = \mu_F \quad \text{and} \quad \frac{|\Delta t_T|}{|\Delta t_N|} > \mu_F \tag{2.24}$$

where Δt_T and Δt_N are the incremental tangential and normal contact components, respectively.

The macro–slip occurs when the shear stress increment Δt_T acting at contact surface exceeds the limiting value of $\mu_F|\Delta t_N|$. To reduce the excess strees an iterative approach suggested by Buczkowski and Altenbach (1989) has been employed. At the next iteration the shear stiffness is calculated by assuming that the same value Δu_T $(= \Delta t_T/k_T)$ exists and the excess of shear stress is reduced to the limiting value as

$$k_T^* = \frac{\text{sign}(\mu_F|\Delta t_N|)}{\Delta u_T} \qquad \begin{cases} \text{sign} = +1 & \text{for} \quad \Delta u_T \geq 0 \\ \text{sign} = -1 & \text{for} \quad \Delta u_T < 0 \end{cases} \tag{2.25}$$

whereas the irreversible macro–slip $\Delta u_T^G = \Delta u_T^p$ is computed by Eq (2.26) given now as

$$\Delta u_T^G = \Delta u_T - \frac{\mu_F|\Delta t_N|}{k_T^e} \tag{2.26}$$

where k_T^e defines the elastic stiffness coefficient. The model is reanalysed until the excess shear stress due to the friction limit becomes zero.

3. Variational formulation

3.1. Incremental description of the contact problem

We have indicated that for an effective numerical treatment of problems involving material nonlinearities and the irreversible nature of friction it is necessary

to use an incremental formulation. We consider the contact problem shown in Fig.2, where V denotes the body in the deformed state, A denotes the surface of V, A_u denotes the part of the surface with a prescribed displacement field $\mathbf{u}$, A_q denotes the part of the surface with a prescribed surface traction $\mathbf{t}$ and A_c denotes the contact zone which is unknown a priori.

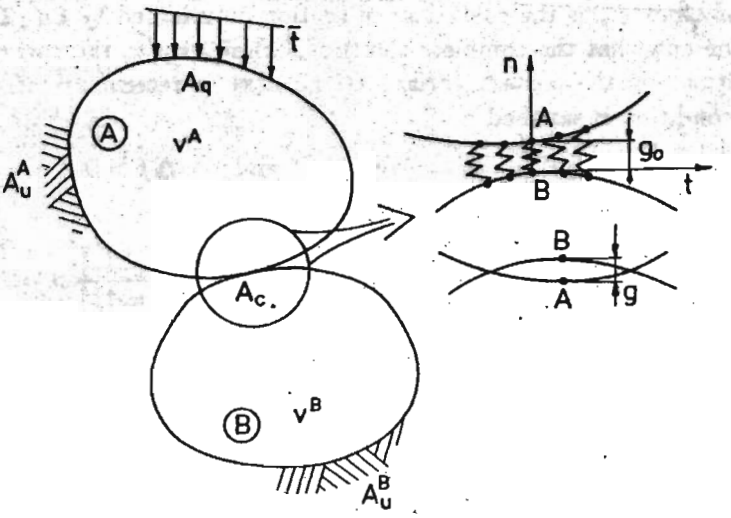

Fig. 2. Contact area for two rough bodies: discrete formulation

For the small deformation elastic–plastic contact problem the fundamental systems of incremental equations can be written in the form of:

— equilibrium equations (intertial effects neglected)

$$\Delta\sigma_{ij,j} = 0 \qquad \text{in} \quad V^A \cup V^B \tag{3.1}$$

where $\Delta\sigma_{ij}$ is Cauchy incremental stress tensor,

— geometric relations

$$2\Delta\varepsilon_{ij} = \Delta u_{i,j} + \Delta u_{j,i} \qquad \text{in} \quad V^A \cup V^B \tag{3.2}$$

where $\Delta\varepsilon_{ij}$ is the incremental strain tensor,

— kinematic boundary conditions (prescribed displacements)

$$\Delta u_i = \Delta \underline{u}_i \qquad \text{on} \quad A_u^A \cup A_u^B \tag{3.3}$$

— static boundary conditions (prescribed boundary tractions)

$$\Delta\sigma_{ij}(u)n_j = \Delta t_i(u) \qquad \text{on} \quad A_q \tag{3.4}$$

$$\left.\begin{aligned} \Delta p_N(u) &= \Delta\sigma_{ij}(u)n_i n_j \\ \Delta \boldsymbol{p}_T(u) &= \Delta \boldsymbol{p}(u) - \Delta p_N \boldsymbol{n} \end{aligned}\right\} \quad i,j = 1,2 \quad \text{on} \quad A_c \tag{3.5}$$

where $\Delta \boldsymbol{p}_T$ and $\Delta \boldsymbol{p}_N$ are tangential (shear) and normal contact tractions; at the contact interface surface the following relationships are valid

$$\begin{aligned} \Delta u_N &= \Delta \boldsymbol{u}\boldsymbol{n} \\ \Delta \boldsymbol{u}_T &= \Delta \boldsymbol{u} - \Delta u_N \boldsymbol{n} \end{aligned} \tag{3.6}$$

— kinematical contact conditions to be specified below.

The current gap g and the contact tractions (contact forces) are related through the inequality conditions

$$\left.\begin{aligned} g &\equiv \left((\boldsymbol{u}^B + \Delta\boldsymbol{u}^B) - (\boldsymbol{u}^A + \Delta\boldsymbol{u})^A\right)\boldsymbol{n} - g_0 \geq 0 \quad \Rightarrow \quad p_N(n)\boldsymbol{n} < 0 \\ g &\equiv \left((\boldsymbol{u}^B + \Delta\boldsymbol{u}^B) - (\boldsymbol{u}^A + \Delta\boldsymbol{u}^A)\right)\boldsymbol{n} - g_0 < 0 \quad \Rightarrow \quad p_N(u)\boldsymbol{n} = 0 \end{aligned}\right\} \quad \text{on} \quad A_c \tag{3.7}$$

g gives the current value of the gap, $\boldsymbol{n}$ represents the unit normal vector, p_N is the contact pressure, Δu is the incremental displacement at the contact surface and g_0 represents the initial gap between the bodies A and B.

In the present work small elastic–plastic deformations have been assumed for both the bodies A and B. Plastic deformations are governed by a yield criterion, a hardening rule and a flow rule, respectively. The post-yield deformation is described by the modification of the yield condition due to a strain-hardening taking place during the plastic flow. The flow rule permits the determination of the plastic strain rate components at each point during the progressive loading history. The yield condition is taken in the Huber–Mises form as

$$f(\sigma_{ij}) = F(\sigma_{ij}^D) - \sigma_Y = \sqrt{3J_2^D} - \sigma_Y = 0 \tag{3.8}$$

where $J_2^D = \sigma_{ij}^D \sigma_{ij}^D$ denotes the second invariant of the deviatoric stress tensor, $\sigma_{ij}^D = \sigma_{ij} - \frac{1}{3}\sigma_{kk}\delta_{ij}$ and σ_Y is the current yield point taken from the uniaxial tension test.

For numerical computations the isotropic linear strain hardening model has been employed (the Bauschinger effect is neglected). After initial yielding the material behaviour is partly elastic and partly plastic. During any increment of stress the changes in strain are assumed to be divisible into elastic and plastic components as

$$\Delta\varepsilon_{ij} = \Delta\varepsilon_{ij}^{(E)} + \Delta\varepsilon_{ij}^{(P)} \tag{3.9}$$

where $\Delta\varepsilon_{ij}^{(E)}$ and $\Delta\varepsilon_{ij}^{(P)}$ stand for the elastic and plastic parts of the total incremental strain, respectively.

For the Hookean material the elastic incremental strain part is assumed to be related to the incremental stress by

$$\Delta\sigma_{ij} = C_{ijkl}^{(E)}\Delta\varepsilon_{ij}^{(E)} \tag{3.10}$$

where $C_{ijkl}^{(E)}$ is the tensor of elastic moduli and the summation convention holds for repeated indicies. The plastic part of the incremental strain is derived from the associated flow rule

$$\Delta\varepsilon_{ij}^{(P)} = \Delta\lambda^P \frac{\partial F}{\partial\sigma_{ij}} \tag{3.11}$$

in which $\Delta\lambda^P$ is a factor of proportionality known as the plastic multiplier.

A number of successive algebric manipulations leads finally to the complete elastic–plastic incremental stress – small strain constitutive relation (Kleiber, 1989)

$$\Delta\sigma_{ij} = C_{ijkl}^{(E-P)}\Delta\varepsilon_{kl} \tag{3.12}$$

in which $C_{ijkl}^{(E-P)}$ is refered to as the elastic–plastic constitutive tensor and can be presented as

$$C_{ijkl}^{(E-P)} = C_{ijst}^{(E)}\left[\delta_{ks}\delta_{lt} - \frac{n_{pr}C_{prkl}^{(E)}n_{st}}{h + n_{pr}C_{prmn}^{(E)}n_{mn}}\right] \tag{3.13}$$

where the indicies i,j,k,l run over 1,2,3, δ_{ij} is the Kronecker delta and n_{ij} represents the unit normal to the yield surface in the stress space as given by (Owen and Hinton, 1986; Kleiber, 1989)

$$n_{ij} = \frac{\frac{\partial F}{\partial\sigma_{ij}}}{\sqrt{\frac{\partial F}{\partial\sigma_{kl}}\frac{\partial F}{\partial\sigma_{kl}}}} = \sqrt{\frac{3}{2}}\frac{\sigma_{ij}^D}{\sigma_Y} \tag{3.14}$$

The module h in Eq (3.13) is a hardening parameter which can be determined experimentally from the uniaxial test data.

3.2. Approximation by the finite element method

The complete solution to the incremental problem described by Eq (3.1) ÷ (3.4) comes down to finding fields of incremental displacements Δu, incremental strains $\Delta\varepsilon$ and incremental stresses $\Delta\sigma$ which satisfy contact conditions (3.5) ÷ (3.7). Adopting the equalibrium state (N) as the reference state for the current state $(N+1)$ (see Fig.3), the increment of the energy functional can be written as

follows (the contact area is treated as given and the loading/unloading properties in both the bodies, interior and the contact area are assumed known)

$$\Delta J_p^{(e)} = \int_{V_A^{(e)} \cup V_B^{(e)}} \Delta\sigma_{ij}\Delta\varepsilon_{ij}dV - \int_{A_q^{(e)}} \Delta u_i^T \Delta t_i dA + \int_{A_c^{(e)}} \Delta p_N^T \Delta u_N dA + \int_{A_c^{(e)}} \Delta p_T^T \Delta u_T dA \tag{3.15}$$

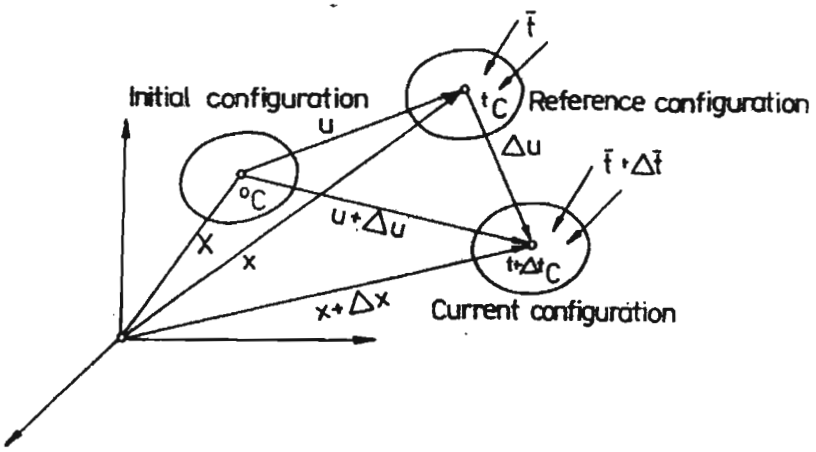

Fig. 3. Actual and reference configuration

Two last terms in Eq (3.15) can be interpreted as fictious energy term representing the influence of the nonlinear Winkler foundation. The upper-index (e) in Eq (3.15) denotes a typical eth finite element and (s) denotes a sth contact element attached to the eth finite element. Substituting constitutive equilibrium (3.12) into Eq (3.15) implies

$$\Delta J_p^{(e)} = \frac{1}{2}\int_{V_A^{(e)} \cup V_B^{(e)}} C_{ijkl}^{(E-P)}\Delta\varepsilon_{ij}\Delta\varepsilon_{kl}dV - \int_{A_q^{(e)}} \Delta u_i^T \Delta t_i dA + \int_{A_c^{(e)}} \Delta p_N^T \Delta u_N dA + \int_{A_c^{(e)}} \Delta p_T^T \Delta u_T dA \tag{3.16}$$

Let us assume now that the functions $\Delta \mathbf{u}$ can be approximated within each element by means of the global shape function matrix $\mathbf{N}$ as

$$\Delta \mathbf{u} = \mathbf{N}\Delta \mathbf{q} \tag{3.17}$$

where $\Delta \boldsymbol{q}$ is the vector of incremental nodal displacements.

Using the incremental matrix form of the strain–displacement relations (3.2) and constitutive equation (3.12)

$$\begin{aligned} \Delta \boldsymbol{\varepsilon} &= \mathbf{D} \Delta \boldsymbol{u} \\ \Delta \boldsymbol{\sigma} &= \mathbf{C}^{(E-P)} \Delta \boldsymbol{\varepsilon} \end{aligned} \tag{3.18}$$

($\mathbf{D}$ denotes the strain operator), the incremental functional (3.10) can be recast into the finite element form as follows

$$\begin{aligned} \Delta J_p^{(e)} = \frac{1}{2} \Delta \boldsymbol{q}^{\mathsf{T}} \int\limits_{V_A^{(e)} \cup V_B^{(e)}} \mathbf{B}^{\mathsf{T}} \mathbf{C}^{(E-P)} \mathbf{B} dV \Delta \boldsymbol{q} - \Delta \boldsymbol{q}^{\mathsf{T}} \Big(\int\limits_{A_q^{(e)}} \mathbf{N}^{\mathsf{T}} \Delta \boldsymbol{t} dA \Big) + \\ + \int\limits_{A_c^{(e)}} \Delta p_N^T \Delta u_N dA + \int\limits_{A_c^{(e)}} \Delta p_T^T \Delta u_T dA \end{aligned} \tag{3.19}$$

where $\mathbf{B} = \mathbf{DN}$ is the (global) strain operator.

For a given contact area A_c the ΔJ_p functional constitutes the basis for the incremental form of the principle of stationary potential energy. The solution $\Delta \boldsymbol{q}$ to the boundary-value problem (3.1) $\div$ (3.7) is given by the stationary conditions of functional (3.19)

$$\delta(\Delta J_p) = \sum_{e=1}^{N} \Big(\frac{\partial(\Delta J_p^{(e)})}{\partial(\Delta \boldsymbol{q})} \Big) \delta(\Delta \boldsymbol{q}) + \sum_{s=1}^{S} \Big(\frac{\partial(\Delta \phi_c)}{\partial(\Delta \boldsymbol{q})} \Big) \delta(\Delta \boldsymbol{q}) = 0 \tag{3.20}$$

where N is the total number of finite elements, S is the total number of contact elements and ϕ_c is written as

$$\Delta \phi_c = \Delta \phi_T + \phi_N = \int\limits_{A_c} \Delta p_N^T \Delta u_N dA + \int\limits_{A_c} \Delta p_T^T \Delta u_T dA \tag{3.21}$$

where A_c is the area of the contact surface corresponding to the contact element (Appendix 1).

Eq (3.20) leads to the following set of nonlinear algebraic equations

$$\Big(\mathbf{K}_{AB}^{(E-P)} + \mathbf{K}_c(\Delta \boldsymbol{q}) \Big) \Delta \boldsymbol{q} = \Delta \boldsymbol{f} - \Delta \boldsymbol{f}_c \tag{3.22}$$

where $\mathbf{K}_{AB}^{(E-P)}$ is the elastic–plastic stiffness matrix given as

$$\mathbf{K}_{AB}^{(E-P)} = \int\limits_{V} \mathbf{B}^{\mathsf{T}} \mathbf{C}^{(E-P)} \mathbf{B} dV \tag{3.23}$$

and Δf the incremental vector of equivalent nodal loads (without the contact nodes) due to applied surface traction which is given as

$$\Delta f = \int_{A_q} \mathbf{N}^{\mathrm{T}} \Delta t dA \tag{3.24}$$

and Δf_c is the incremental vector of contact forces which is obtained from the last two integrals in (3.15). The Δf_c is expressed as the sum of the tangential and normal contact forces as

$$\Delta f_c = \int_{A_c} \delta k_N \Delta u_N dA + \int_{A_c} \delta k_T \Delta u_T dA \tag{3.25}$$

Assuming infinitesimal increments of Δp_N and Δp_T expressed by (3.26) as

$$\Delta p_N = \frac{\partial p_N}{\partial u_N} \Delta u_N \qquad \Delta p_T = \frac{\partial p_T}{\partial u_T} \Delta u_T \tag{3.26}$$

the relationship (3.21) can be rewritten as follows

$$\begin{aligned} \Delta \phi_T &= \frac{1}{2} \int_{A_c} \left[\left(\frac{\partial p_T}{\partial u_T} \Delta u_T \right)^{\mathrm{T}} \Delta u_T \right] dA = \frac{1}{2} k_T \int_{A_c} \Delta u_T^{\mathrm{T}} \Delta u_T dA \\ \Delta \phi_N &= \frac{1}{2} \int_{A_c} \left[\left(\frac{\partial p_N}{\partial u_N} \Delta u_N \right)^{\mathrm{T}} \Delta u_N \right] dA = \frac{1}{2} k_N \int_{A_c} \Delta u_N^{\mathrm{T}} \Delta u_N dA \end{aligned} \tag{3.27}$$

where $k_T = \frac{\partial p_T}{\partial u_T}$ = constant (see Fig.1) and $k_N = \frac{\partial p_N}{\partial u_N}$ expressed by means of Eq (2.7) denote the coefficients of the contact stiffness matrix in tangential and normal directions, respectively.

By substituting Eq (3.17) into Eqs $(3.27)_1$ and $(3.27)_2$ we arrive at

$$\begin{aligned} \Delta \phi_T &= \frac{1}{2} k_T \Delta q_T^{\mathrm{T}} \left[\int_{A_c^{(e)}} \mathbf{N}^{\mathrm{T}} \mathbf{N} dA \right] \Delta q_T \\ \Delta \phi_N &= \frac{1}{2} k_N \Delta q_N^{\mathrm{T}} \left[\int_{A_c^{(e)}} \mathbf{N}^{\mathrm{T}} \mathbf{N} dA \right] \Delta q_N \end{aligned} \tag{3.28}$$

The formula given by direct integration for typical C^0 shape functions (quadratic of eight-node serendipity element) evaluates the consistent contact matrix which has the full rank, cf. the consistent-mass matrix computation, as

$$\int_{A_c^{(e)}} \mathbf{N}^{\mathrm{T}} \mathbf{N} dA = \frac{A_c^{(e)}}{30} \begin{bmatrix} 4 & 2 & -1 \\ 2 & 16 & 2 \\ -1 & 2 & 4 \end{bmatrix} \tag{3.29}$$

Some of the algorithms become more efficient if one of the global matrices can be diagonalized (lumped) (Zienkiewicz, Taylor, 1989). In practice, the diagonal or lumped matrices are often employed due to their economy and because they lead to some particularly attractive time integration schemes (so–called explicit methods) (Hughes, 1987). Besides, the diagonalized matrix has often clear physical interpretation. There are several ways of forming lumped matrices. One of them is to employ the row–sum technique (Hughes, 1987, Zienkiewicz and Taylor, 1989). The name originates from the fact that it is based on the relation

$$a_{ij}^{(s)} = \begin{cases} \sum_r \int_{A_c} N_i^T N_r dA = \int_{A_c} N_i^T \sum_r N_r dA = \int_{A_c} N_i^T dA & \text{for } i = j \\ 0 & \text{for } i \neq j \end{cases} \tag{3.30}$$

in which $\sum_r N_r = 1$, where r is the number of the element nodes, N_r is the rth shape function and s is the number of the contact element. This algorithm employs the diagonal sum of all terms in a given row.

Differentiation of Eq (3.28) and the use of the lumped matrix Eq (3.31) via Eq (3.30) leads to the stiffness matrix of a single contact element for the tangential and normal directions, respectively as

$$\mathbf{K}_{c(T)}^{(s)} = \frac{\partial \phi_T}{\partial \Delta \boldsymbol{q}_T} = \frac{(\Delta p_N)^S}{R} \frac{A_c^{(s)}}{30} \begin{bmatrix} 5 & 0 & 0 \\ 0 & 20 & 0 \\ 0 & 0 & 5 \end{bmatrix}$$

$$\mathbf{K}_{c(N)}^{(s)} = \frac{\partial \phi_N}{\partial \Delta \boldsymbol{q}_N} = \frac{(\Delta p_N)^{1-m}}{c_N m} \frac{A_c^{(s)}}{30} \begin{bmatrix} 5 & 0 & 0 \\ 0 & 20 & 0 \\ 0 & 0 & 5 \end{bmatrix} \tag{3.31}$$

c_N, m, R, S being the coefficients defined in section 2 and $A_c^{(s)}$ is the area of contact surface along three contact spring elements (see Appendix).

The submatrix (3.29) can be used in order to obtain the stiffness matrix for the six–node bond–contact element. Because the contact stiffness matrix so–obtained depends directly on the incremental contact pressure Δp_N it is here assumed that constant contact pressure p_N changes in each spring–contact element. The spring–contact elements can describe the nonlinear behaviour at the interface of surface more accurately. When using the bond–contact elements the contact pressure along the bond contact element must be assumed and, therefore, a more refined mesh discretization of the contact zone is required.

The discretized area of contact surface for the isoparametric elements can be expressed as

$$A_c = \int_{-1}^{+1} \int_{-1}^{+1} \det[j] d\xi d\eta \tag{3.32}$$

where $\det[j]$ is the jacobian determinant and ξ, η are the natural coordinates for quadrialateral element. The stiffness matrix of three spring–contact elements is given in the appendix.

4. Solution algorithm

An iterative procedure must be employed for solving the incrementally nonlinear problem of elastic–plasticity at any stage of the deformation process. If we consider a typical load increment $m+1$, at the beginning of which the state is characterized by a set of known nodal displacement parameters Δu_m and stresses $\Delta\sigma_m$ producing the internal nodal forces Δf_m, we can write a set of nonlinear algebraic equations for the $m+1$ step in the following form [Zienkiewicz, 1977]

$$\Delta\psi^n_{m+1} \equiv \Delta R_{m+1} - \left(\Delta f^n_{m+1} + (\Delta f_c)^n_{m+1}\right) \tag{4.1}$$

where $\Delta\psi^n_{m+1}$ is the residual or unbalanced nodal force vector, m is the load increment number, n is the iteration number at the mth load increment, ΔR_{m+1} is the vector of eqiuvalent nodal loads from applied surface tractions, $(\Delta f_c)^n_{m+1}$ is the increment of the nodal contact forces, Δf^n_{m+1} is the increment of the equivalent internal nodal forces related to the element stresses by

$$\Delta f^n_{m+1} = \int \mathbf{B}^{\mathsf{T}} \Delta\sigma^n_{m+1} dV \tag{4.2}$$

To obtain an improved solution the first order Taylor expansion is made yielding

$$\Delta\psi^{n+1}_{m+1} = \Delta\psi^n_{m+1} + \frac{\partial(\Delta\psi^n_{m+1})}{\partial(u^n_{m+1})}\Delta u^n_{m+1} \doteq 0 \tag{4.3}$$

Using the relations (4.1) and (4.3) we can write

$$\Delta\psi^{n+1}_{m+1} = \left[\Delta R_{m+1} - \left(\Delta f^n_{m+1} + (\Delta f_c)^n_{m+1}\right)\right] - (\mathbf{K}_T)^n_{m+1}\Delta u^n_{m+1} = 0 \tag{4.4}$$

where n is the nth successively updated tangent stiffness matrix for the $m+1$ load increment which, by using Eq (4.1), can be expressed as

$$(\mathbf{K}_T)^n_{m+1} = \frac{\partial(\Delta\psi^n_{m+1})}{\partial(u^n_{m+1})} = \frac{\partial\left(\Delta f^n_{m+1} + (\Delta f_c)^n_{m+1}\right)}{\partial(u^n_{m+1})} \tag{4.5}$$

or, in a more compact form, as

$$(\mathbf{K}_T)^n_{m+1} = \left[(\mathbf{K}^{E-P}_{AB})^n_{m+1} + (\mathbf{K}_C)^n_{m+1}\right] \tag{4.6}$$

where the first term in Eq (4.6) stands for the elastic–plastic stiffness matrix (Eq3.22) and the second term denotes the contact stiffness matrix (Eqs $(3.31)_1$ and $(3.31)_2$).

The value of $\Delta \mathbf{u}^n_{m+1}$ from Eq (4.4) is used to determine an improved displacement estimate after the $n+1$ iteration at the $m+1$ load increment as

$$\mathbf{u}^{n+1}_{m+1} = \mathbf{u}^n_{m+1} + \Delta \mathbf{u}^n_{m+1} \tag{4.7}$$

Different modifications to the above algorithm, such as the so–called modified Newthon–Raphson algorithm or the initial load algorithm or the initial load algorithm, based on the elastic stiffness matrix, have been implemented in the program used to compute the example described below. The use of the algorithm based on the constant elastic stiffness matrix has proved to be the most economical for this problem (the shortest computational time), even though the convergence for this algorithm has been the slowest. In this algorithm the relation (4.6) is replaced by

$$(\mathbf{K}_T)^n_{m+1} = \left[(\mathbf{K}^E_{AB})^0 + (\mathbf{K}_C)^n_{m+1}\right] \tag{4.8}$$

Independently of this build–up of the "tangent" stiffness matrix the modification of the contact matrix in accordance with the contact condition (3.7) and the elastic–plastic friction model (see section 2) is employed at each iteration.

5. Numerical example

The example to be discussed is taken from Lee and Kwak (1984). An elastic (or elastic–plastic) punch A is pressed against an elastic–plastic foundation B as shown in Fig.4. A uniform pressure $\bar{t}$ is applied to the upper face of the body A. The actual external forces are scaled by dividing them respectively by their values corresponding to the initiation of the plastic deformation. The material of the body B is assumed to be elastic–plastic with the yield stress σ^B_Y of 196 [MPa]; the yield stress σ^A_Y of the body A is assumed to be 1960 [MPa]. The elastic modulus for both the bodies is assumed to be 206 [GPa] while the Poisson ratio is 0.3. The problem is solved under both the plane stress and the plane strain conditions. Because of the symmetry only one half of each body is considered. The appropriate kinematic boundary constraints are imposed on the axis of symmetry. Numerical results were compared to the results of Lee and Kwak (1984) by neglecting the tangential behaviour at the contact surface and assuming $c_N = 0.001$ and $m = 0.5$.

Fig.5 shows the load ratio r versus displacement at the centre of the contact region for both the plane stress and plane strain cases. The load–displacement curve from Fig.5 for the plane stress has a sharp bend at the load ratio $r = 1.42$

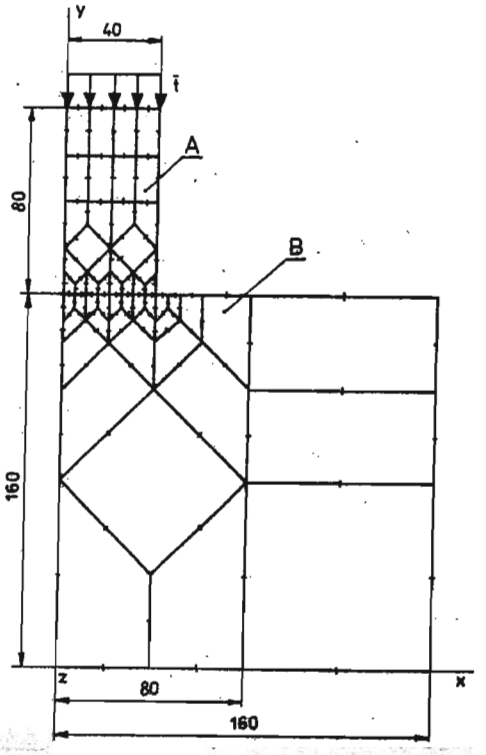

Fig. 4. Elastic intendor pressed against a rough elastic–plastic foundation. Initial finite element mesh consists of eight nodal elements of serendipity family

($r = 1.34$ according to Lee and Kwak). For the plane stress situation the plastic yielding begins at the contact surface in the element situated close to the edge of the intendor A. The total load corresponding to the first yielding is 7.17 [kN] per unit thickness (the value given by Lee and Kwak is 7.07 [kN]). Under the plane strain conditions the yielding starts at the load of 9.75 [kN] (the value of 9.73 [kN] was obtained by Lee and Kwak). Taking into account the tangential behaviour yielding for the plane stress problem begins at the load of 7.00 [kN]. The contact pressure distribution for different external load levels for the plane stress problem is shown in Fig.6a and 6b. It is seen that the contact pressure distribution is uniform at higher loads. For the plane strees problem the mean contact pressure is found not to exceed the value of 240 [MPa]. According to Kachanov (see Lee and Kwak Lee and Kwak, 1984) the maximum resistible load is $(2/\sqrt{3})\sigma_Y = 221$ [MPa].

Assuming $c_N = 0.001$ and $m = 0.5$ this plane stress example was next

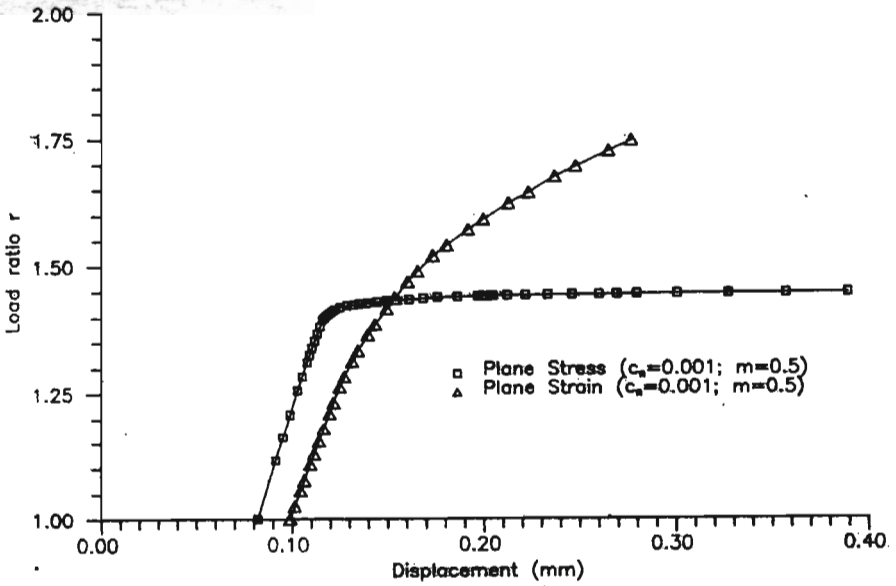

Fig. 5. Load–displacement characteristics of the center contact node for plane stress problem ($r = 1.0$ for external load 7.17 [kN]) and for plane strain problem ($r = 1.0$ for external load 9.75)

considered to test the frictional interface law. The parameters β, n and k_T^P (see section 2) are given in Fig.7. Fig.7a, 7b and 7c show the tangential contact stress distributions along the contact surface. It is seen that the increase of the external load results in the decrease of the tangential contact pressure; moreover, the shear contact tractions change sign at some contact nodes. It was also found that in the plastically deformed region of the bodies the shear contact pressure p_T did not exceed the friction forces $\mu_F|p_N|$ that had been observed in the elastic deformed state. By using the elastic–plastic friction model ($k_T^p \neq k_T^e$) the decrease of the shear contact forces was found. This can be explained by observing that with an increase of the external forces after initiation of the plastic deformation a decrease of the shear influence in the contact zone takes place along with the effect of the contact pressure distribution becoming more and more uniform. It can be said that this phenomenon is strongly related to the the plastic deformation of the foundation B.

Fig.8 shows the deflection of the upper surface of the body B versus the hardening parameter h for the plane stress problem. With the increase of the parameter h the overall hardening of the elastic–plastic foundation can be observed.

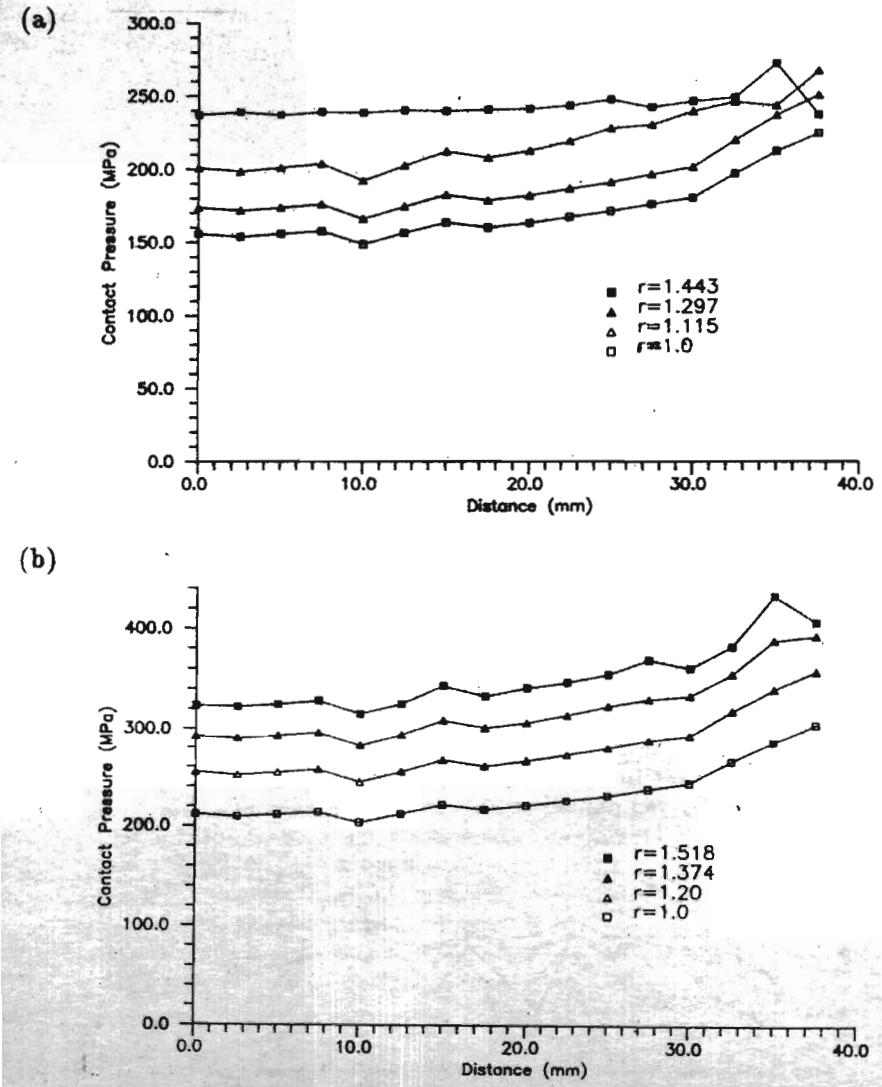

Fig. 6. Contact pressure distribution for different external load levels ($c_N = 0.001$ and $m = 0.5$); (a) – plane stress problem, (b) – plane strain problem

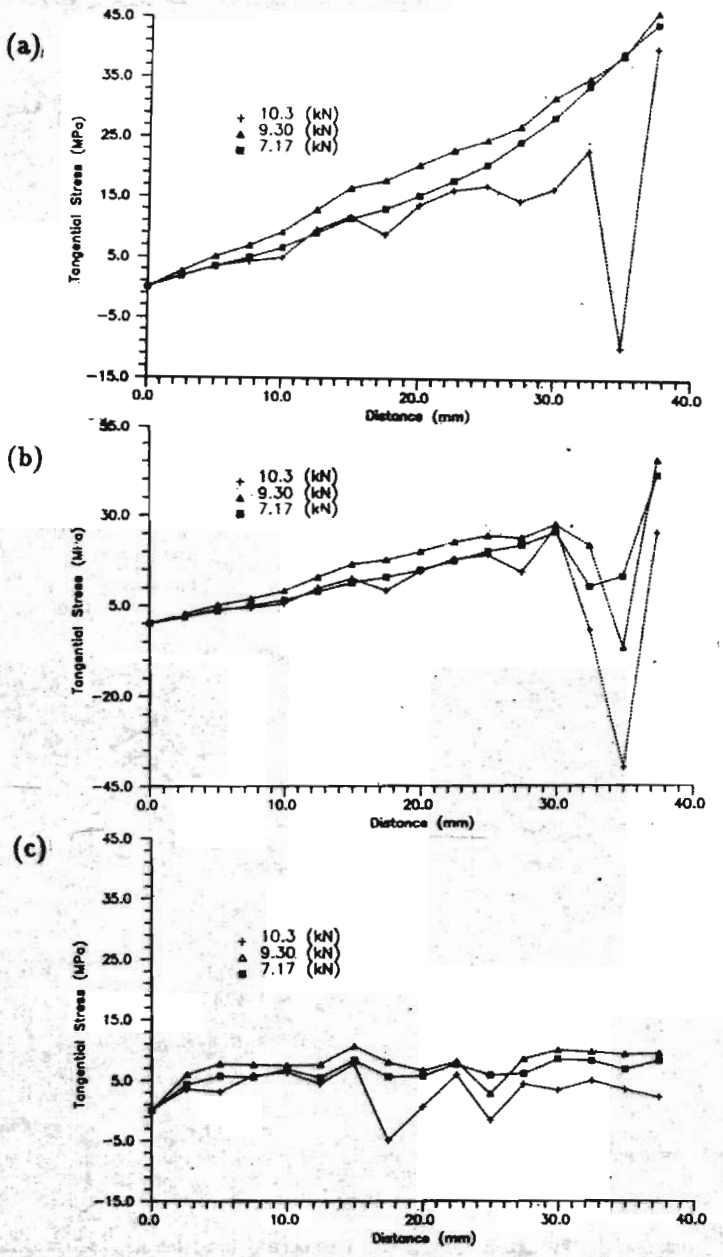

Fig. 7. Tangential contact distribution for different external load levels, plane stress problem, $c_N = 0.001$, $m = 0.5$;
(a) $k_T^{(p)} = 1.0 k_T^{(e)}$, $R = 0.9$, $S = 0.5$, $\mu = 0.2$, $\beta = 1.0$, $n = 275$ [1/mm],
(b) $k_T^{(p)} = 0.05 k_T^{(e)}$, $R = 0.9$, $S = 0.5$, $\mu = 0.2$, $\beta = 1.0$, $n = 275$ [1/mm],
(c) $k_T^{(p)} = 0.05 k_T^{(e)}$, $R = 0.9$, $S = 0.5$, $\mu = 0.2$, $\beta = 0.2$, $n = 275$ [1/mm]

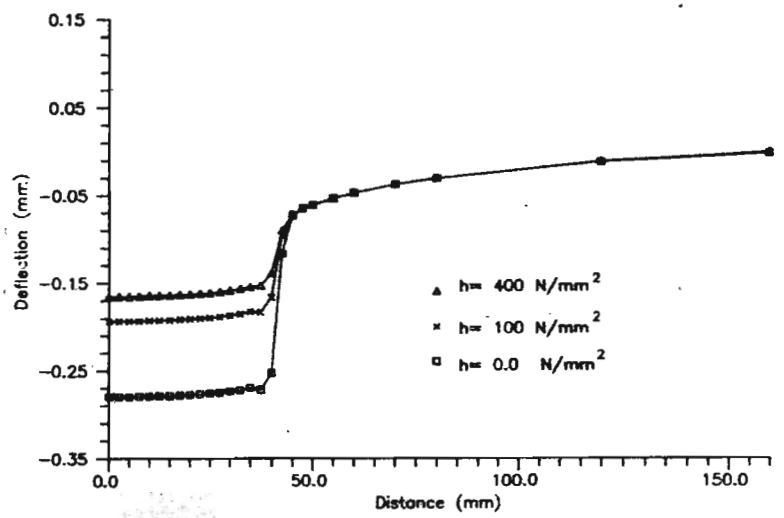

Fig. 8. Deflection of the upper surface of the elastic–plastic foundation versus the hardening plastic parameter h for the plane stress problem, $c_N = 0.001$, $m = 0.5$. Total external load equals 10.35 [kN]

6. Conclusions

The following conclusions can be drawn from the analysis performed

1. in the plane stress problem the plastic yielding occurs on the contact surface starting at the edge of the intendor. Under the plane strain condition yielding begins at higher external forces and it does not begin at the edge of the intendor but a few mm off the outer surface,

2. in the plane stress identation problem plastic enclaves spreads at a slower rate,

3. taking account of the tangential contact compliance results in a decrease of the contact pressure close to the sharp edge of the intendor (singular point),

4. accounting for the tangential contact compliance results in an elastic–plastic foundation yielding at smaller external loads,

5. friction implies a smaller pressure gradient near the singular point,

6. tangential contact stresses in the plastically deformed region decrease along with an increasing external load.

References

1. ALTENBACH J., BUCZKOWSKI R., 1991, *Finite-Elemente Modellierung 2D-Kontaktproblems*, Technische Mechanik, **12**, 2, 93-106
2. BACK N., BURDEKIN N., COWLEY A., 1972, *Review of the research on fixed and sliding joints*, 87-97, in: (Eds.A.Tobias and F.Koenigsberger), Proc. 13th Internat. Machine Design and Research Conf., London
3. BACK N., BURDEKIN N., COWLEY A., 1973A, *Analysis of machine tool joints by the element method*, 529-537, in: (Eds.A.Tobias and F.Koenigsberger), Proc. 14 th. Internat. Machine Design and Research Conf., London
4. BACK N., BURDEKIN M., COWLEY A., 1973B, *Pressure distribution and deformations of machined components in contact*, Int.J.Mech.Sci., **15**, 993-1010
5. BLOCH M.W., OROBINSKI M.W., 1983, *O modifikacii metoda konečnykh elementov dlya rešeniya dvukhmiernykh uprugikh i plastičeskikh kontaktnykh zadači*, Problemy Pročnosti, 5, 21-27
6. BUCZKOWSKI R., ALTENBACH J., 1989, *Numerische Berechnung zweidimensionaler Kontaktaufgaben mit Berücksichtigung der nichtlinearen Eigenschaften der Kontaktzone*, Technische Mechanik, **10**, 3, 183-196
7. CHENG J.H., KIKUCHI N., 1985A, *An Anaysis of Metal Forming Processes Using Large Deformation Elastic-Plastic Formulations*, Comp.Meth.in Appl. Mech.Engng., **49**, 71-108
8. CHENG J.H., KIKUCHI N., 1985B, *An Incremental Constitutive Relation of Unilateral Contact Friction for Large Deformation Analysis*, J. of Appl.Mech., **52**, 639-648
9. CONNOLY R., THORNLEY R.H., 1968, *Determining the normal stiffnes of joint faces*, J.of Eng.for Industry Feb., 97-106
10. CHVOROSTUCHIN L.A., ŠIŠKIN W., 1980, *Ob osesimmetričnom kontakte dvukh tolstostvennykh oboloček s učetom serekhovosti posadočnykh poverkhnosti*, Mašinostroenie, 2, 5-11
11. CHVOROSTUCHIN L.A., ŠIŠKIN W., USTINOV W.D., 1981 *Vliyanie formy posadočnykh poverkhnosti na raspredelenie kontaktnykh napraženi ˘ i w pressovykh soedineniyakh*, Mašinostroenie, 8, 7-11
12. COURTNEY-PRATT J., EISNER E., 1957, *The effect of a tangential force on the contact of metallic bodies*, Proc.Roy.Soc.A, **238**, 529-550
13. FREDRIKSSON B., 1975, *Experimental determination frictional properties in araldite b contacts*, Report LiTH-IKP-R-061, Linköping Institute of Technology
14. FREDRIKSSON B., *Finite element solution of surface nonlinearities in structural mechanics with emphasis to contact and fracture mechanics problems*, Comp. & Struct., 6, 281-290
15. GABBERT U., 1987, *Die Finite-Element-Methode in dem Ingenieurwissenschaften unter dem Aspekt der rechentechnischen Realisierung im Rahmen universeller Programmsysteme*, Habilitation, Technische Universität Magdeburg
16. HUGHES T.J.R., 1987, *The Finite Element Method. Linear Static and Dynamic Finite Element Analysis*, Prentice-Hall Inc., New Jersey
17. KAWIAK R., 1984, *Wyznaczenie i analiza naprężeń i przemieszczeń w złączu śrubowym*, Praca doktorska, Politechnika Szczecińska

18. KIRSANOVA V.N., 1967, *The Shear Compliance of Flat Joints*, Machines and Tooling, **38**, 7, 30-34

19. KLARBRING A., 1986, *The Influence of Slip and Interface on Contact Stress Distributions. A Mathematical Programming Approach*, in: Mechanics of Material (eds. A.P.Selvaduari & G.Z.Voyiadjis), Elsevier, Amsterdam, 43-59

20. KLARBRING A., MIKELIĆ A., SHILLOR M., 1988, *Frictional Contact Problems with Normal Compliance*, Int.J.Engng.Sci., **26**, 8, 811-832

21. KLARBRING A., 1990, *Derivation and analysios of rate boundary-value problems of frictional contact*, Eur.J.Mech., A/ Solids, **9**, 1, 53-85

22. KLEIBER M., 1989, *Incremental finite element modelling in non-linear soild mechanics*, PWN Warszawa/Ellis Horwood Chichester

23. KOIZUMI T., ITO Y., MASUKO M., *Experimental Expression of the Tangential Micro-displacement between Joint Surfaces*, Bull.of the JSME, **22**, 166, 591-597

24. KOPS L., ADAMS D.H., 1984, *Effect of shear stiffnes of fixed joints on thermal deformation of machine toos*, Annals of CIRP, **33**, 1, 233-238

25. LEE B.C., KWAK B.M., 1984, *A computational method for elasto-plastic contact problems*, Comp. & Struct., **18**, 5, 757-765

26. LEVINA Z.M., 1967, *Research on the static stiffnes of joints in machine tools*, Proc. 8th Internat. Machine Design and Research Conf., London, 737-756

27. LINDGREN M., 1973, *Drehmomentübertragung in Preß-verbindungen*, Konstruktion, **25**, 338-441

28. MARTINS J.A.C., ODEN J.T., 1986, *Interface Models, Variational Principles and Numerical Solutions for Dynamic Friction Problems*, in: Mechanics of Material (eds. A.P.Selvaduari & G.Z.Voyiadjis), Elsevier, Amsterdam, 3-23

29. MARTINS J.A.C., ODEN J.T., SIMOES F.M.F., 1990, *A study of static and kinematic friction*, Int.J.Engng.Sci., **28**, 1, 29-92

30. MORAWSKI A., RAKOWSKI W., SKALSKI K., 1986, *Deformacja sprężysto-plastyczna podczas kontaktu wierzchołków mikro-nierówności*, ZEM, **65**, 1, 19-29

31. MASUKO M., ITO Y., KOIZUMI T., 1974, *Horizontal stiffness and microslip a bolted joint subjected to repeated static loads*, Bull.of the JSME, **17**, 113, 1494-1501

32. MÜLLER K., 1975, *Prediction of the occurence of wear by friction. Force-displacement curves*, WEAR **34**, 439-447

33. ODEN J.T., MARTINS J.A.C., 1985, *Models and computational methods for dynamic friction phenomena*, Comp.Meth.in Appl.Mech.Engng., **52**, 527-634

34. OWEN D.R.J., HINTON E., 1986, *Finite Elements in Plasticity: Theorie and Practice*, Pinerigde Press, Swansea, UK

35. PLESHA M., BELYTSCHKO T., 1986, *On the Modeling of Contact Problems with Dilation*, in: Mechanics of Material (eds. A.P.Selvaduari & G.Z.Voyiadjis), Elsevier, Amsterdam, 63-77

36. RABIER P., MARTINS J.A.C., ODEN J.T., CAMPOS L., 1986, *Existence and local uniqueness of solution to contact problems in elasticity with nonlinear friction laws*, Int.J.Engng.Sci., **24**, 11, 1755-1768

37. REŠETOV D.N., KIRSANOVA V.I., 1976, *Kasatel'naya kontaktnaya podatlivost' detale˘ i*, Mašinovedenie, 2, 88-101

38. SALAMON N.J., TONG X.X., MAHMOUD F.F., 1985, *Effects of profile, roughness and friction on contacting bodies in compression*, WEAR, (101), 205-218

39. SKALSKI K., 1988, *Zagadnienia kontaktowe w zakresie sprężysto–plastycznym*, in: Mechanika kontaktu powierzchni (ed. Z.Mróz), IPPT PAN, Ossolineum, Wrocław, 211-273

40. TANGENA A.G., WIJNHOVEN P.J.M., 1985, *Finite Element Calculations on the Influence of Surface Roughness on Friction*, WEAR, (103), 345-354

41. TANIGUCHI A., TSUTSUMI M., ITO Y., 1984, *Treatment of Contact Stiffness in Structural Analysis*, Bull.of the JSME, 27, 225, 601-607

42. THORNLEY R.W., ELEWA I., 1988, *The static and dynamic stiffness of interference shrink–fitted joints*, Int.J.Mach.Tools Manufact., 28, 2, 141-155

43. VILLANUEVA–LEAL A., HINDUJA S., 1984, *Modelling the characteristics of interface by the finite element method*, Proc.Inst.Mech.Engrs., 198C, 4, 9-23

44. WRIGGERS P., 1987, *On consistent tangent matrices for frictional contact problems*, Proceed.of the Conf.NUMETA 87, Swansea, C15/1-C15/8

45. WRIGGERS P., VU–VAN T., STEIN E., 1990, *Finite–Element–Formulation of Large Deformation Impact- Contact- Problems with Friction*, Comp.& Struct., 37, 3, 319-331

46. YAMADA A., KAKUBARI T., 1988, *The Estimation of Dynamic Charakteristics of a Beam with Junction*, Bull.Japan Soc.of Prec.Engng., 22, 1, 18-24

47. ZIENKIEWICZ O.C., 1977, *The Finite Element Method*, (3 rd. Edition), McGraw–Hill, London

48. ZIENKIEWICZ O.C., TAYLOR R.L., 1989, *The Finite Element Method, vol.I: Basic Formulation and Linear Problems*, McGraw–Hill, London

Appendix

Contact stiffness matrix $\mathbf{K}_c$ for the plane problem

$$\mathbf{K}_c = \frac{A_c}{30}\cdot$$

$$\begin{bmatrix}
5k_T^I & 0 & 0 & 0 & 0 & 0 & -5k_T^I & 0 & 0 & 0 & 0 & 0 \\
 & 5k_N^I & 0 & 0 & 0 & 0 & 0 & -5k_N^I & 0 & 0 & 0 & 0 \\
 & & 20k_T^{II} & 0 & 0 & 0 & 0 & 0 & -20k_T^{II} & 0 & 0 & 0 \\
 & & & 20k_N^{II} & 0 & 0 & 0 & 0 & 0 & -20k_N^{II} & 0 & 0 \\
 & & & & 5k_T^{III} & 0 & 0 & 0 & 0 & 0 & -5k_T^{III} & 0 \\
 & & \text{SYM.} & & & 5k_N^{III} & 0 & 0 & 0 & 0 & 0 & -5k_N^{III} \\
 & & & & & & 5k_T^I & 0 & 0 & 0 & 0 & 0 \\
 & & & & & & & 5k_N^I & 0 & 0 & 0 & 0 \\
 & & & & & & & & 20k_T^{II} & 0 & 0 & 0 \\
 & & & & & & & & & 20k_N^{II} & 0 & 0 \\
 & & & & & & & & & & 5k_T^{III} & 0 \\
 & & & & & & & & & & & 5k_N^{III}
\end{bmatrix}$$

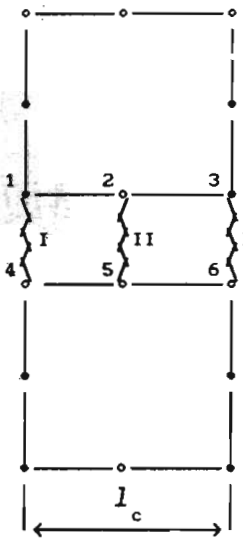

I- Element number 1
II- Element number 2
III- Element number 3

A_c is the contact area corresponding to three contact spring elements; for the plane stress problem $A_c = l_c t$, where t is the thickness and l_c is the lenght of the contact segment.

Sprężysto–plastyczna analiza płaskiego zagadnienia kontaktowego z uwzględnieniem podatności stykowej metodą elementów skończonych

Streszczenie

W pracy przedstawiono rozwiązanie sprężysto–plastycznego dwuwymiarowego zagadnienia kontaktowego z uwzględnieniem deformacji mikronierówości na powierzchni styku. Zagadnienie sformułowano w postaci przyrostowego funkcjonału wariacyjnego w ujęciu przemieszczeniowym i aproksymowano metodą elementów skończonych. Do symulacji nieliniowych właściwości na powierzchni styku zastosowano specjalny element kontaktowy złożony z trzech dyskretnych elementów sprężynowych, których sztywności określono w oparciu o doświadczalne charakterystyki podatności stykowej powierzchni chropowatych. Poprawność zaprezentowanego algorytmu potwierdzono przykładem obliczeniowym. Przedstawiono wpływ parametrów określających sztywność kontaktową na rozkład naprężeń i przemieszczeń na powierzchni kontaktu.

Manuscript received May 13, 1991; accepted for print April 20, 1992